INL/EXT-10-20664

Multi-Collector Isotope Ratio Mass Spectrometer – Operational Performance Report

A.D. Appelhans
J. E. Olson
M. G. Watrous
M. B. Ward
D. A. Dahl

December 2010

The INL is a U.S. Department of Energy National Laboratory
operated by Battelle Energy Alliance

INL/EXT-10-20664

Multi-Collector Isotope Ratio Mass Spectrometer – Operational Performance Report

A.D. Appelhans
J.E. Olson
M.G. Watrous
M.B. Ward
D.A. Dahl

December 2010

Idaho National Laboratory
Idaho Falls, Idaho 83415

http://www.inl.gov

Prepared for the
U.S. Air Force
and for the
U.S Department of Energy
Under DOE Idaho Operations Office
Contract DE-AC07-05ID14517

ABSTRACT

This report describes the operational testing of a new magnetic sector mass spectrometer that utilizes seven full-sized discrete dynode electron multipliers operating simultaneously. The instrument includes a newly developed ion dispersion lens that enables the mass dispersed individual isotope beams to be separated sufficiently to allow a full-sized discrete dynode pulse counting multiplier to be used to measure each isotope beam. The performance of the instrument was measured using SRM 996 (^{244}Pu spike) at loadings of 2.4 and 12 fg on resin beads and with SRM 4350B Columbia River Sediment samples. The measured limit of detection (3σ) for ^{240}Pu was 3.4 attograms for SRM 996. The limit of quantitation, defined as 10 σ, was 11.2 attograms. The measured concentration of ^{239}Pu in the CRS standard was 152 ± 6 fg/g.

CONTENTS

Introduction

The measurement of isotope ratios of actinides at trace levels in environmental samples presents a significant challenge to mass spectrometry. Historically such measurements were made via thermal ionization with multi-sector instruments incorporating a single pulse counting detector system using either a discrete dynode electron multiplier or a Daly detector[1]. Peak stepping was employed to cover the range of isotopes required with some form of mass-fractionation correction. The development of multi-collector magnetic sector instruments offered a means for increasing the sensitivity, accuracy and precision of these measurements by avoiding the dead time associated with peak stepping and the need for mass fractionation corrections (when the total evaporation method was employed). Wieser and Schwieters[2] provide a comprehensive description of the development of multiple collector isotope ratio mass spectrometry. In the commercial multi-collector instruments available today various types of electron multipliers coupled to pulse counters are used to detect extremely low level signals. However, the space constraints at the focal plane of the instruments have limited the number or type of electron multipliers that can be used. Nu instruments[3] employ discrete dynode multipliers, but are limited to 3; IsotopX[4] (formerly GV) and Thermo-Scientific[5] utilize miniaturized channel electron multipliers and some full sized detectors on selected channels. With the goal of further improving the limit of detection of multi-collector instruments we have developed an ion-optical configuration that enables simultaneous measurement of up to 7 isotopes using full-sized discrete dynode electron multipliers. The instrument has been described in detail in a previous report[6]; it was specifically designed for analyzing attogram levels of Pu using the resin bead technique. In this report we present an overview of the instrument design followed by the measured isotope ratios and sample utilization efficiency for over 100 samples of the ^{244}Pu standard spike SRM 996 at several levels and for 15 samples of the Columbia River Sediment standard SRM 4350B. The objective of these measurements was to demonstrate the performance of the instrument for ultra trace level samples. This report does not include in any detail the methods used for chemical separation of the samples.

Ion Optical Design

The instrument is based on a traditional single magnetic sector design utilizing off-normal entrance and exit poles to extend the focal length, increase the dispersion and provide Z focusing. A unique ion lens, which we call an electrostatic dispersion lens[7,8] (EDL), is used to provide the additional separation of the ion beams needed to accommodate the full sized discrete dynode detectors. The thermal ionization ion source and acceleration lens is based on a previous design[9] with high transmission efficiency. The instrument was designed using the SIMION 3D[10] ion optics modeling software. Figure 1 shows the full instrument ion optics model and a set of ion trajectories.

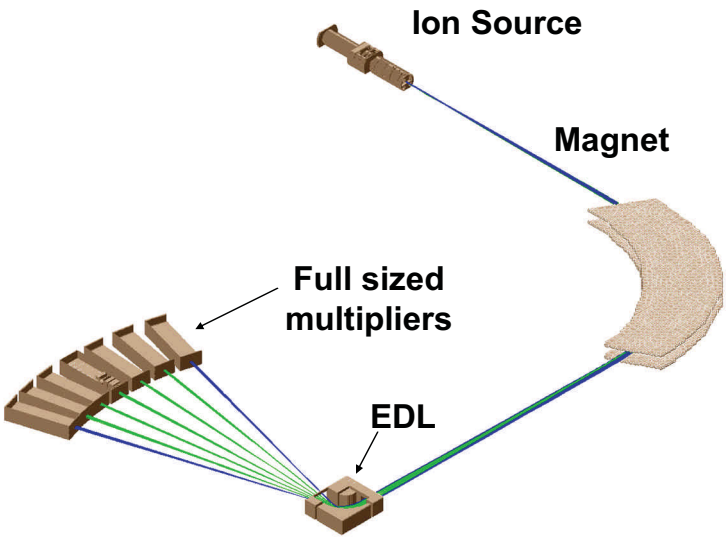

Figure 1 Isometric view of the SIMION ion optical model of the instrument.

Ion source and accelerating lens

The ion source and accelerating lens design is a derivative of the univoltage ion gun developed previously at the INL[9]. A cross section of the lens is shown in Figure 2 and a cut-away 3-D view in Figure 3. The filaments are made in-house out of zone-refined Re ribbon; the face of the filament holding the sample is 1.2 mm square; the filament face sits in a 2 mm diameter aperture. The aperture plate voltage can be biased +/- 20 volts with respect to the filament voltage, which is 5 kV. The focus aperture is at ground potential. The Einzel lens can be used to adjust the focal point of the ion beam; it is normally operated at ground potential. The X and Z deflectors operate between ±20 volts. A second set of X and Z deflectors are located approximately midway between the ion source and the magnet. Figure 4 shows a set of ion trajectories for an ion emission area of 0.2 mm, typical size of a resin bead.

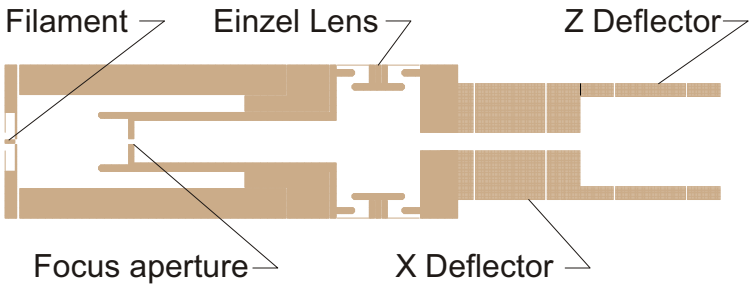

Figure 2 Cross-section view of the univoltage ion gun with X and Z deflectors.

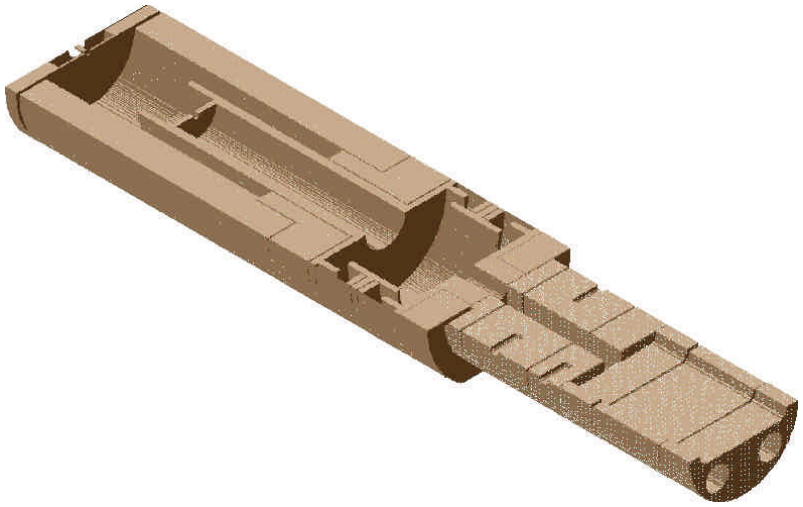

Figure 3 Cut-away view of the ion source and accelerating lens with X and Z deflectors.

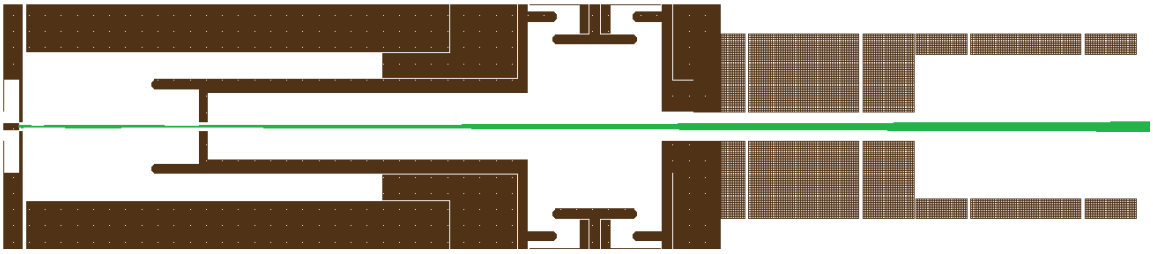

Figure 4 Ion trajectories from a 0.2 mm emission area.

Magnet

The ion optical design of the wide dispersion mass spectrometer includes a single magnetic sector based on a standard VG[11] magnet with non-normal entry and exit poles, the exit pole angle being adjustable. This magnet configuration, referred to as the double dispersion geometry, provides the maximum dispersion of the ion beams at the focal plane and also focuses the beams in the Z plane.

Electrostatic Dispersion Lens

The electrostatic dispersion lens (EDL), invented[6] at the INL, is a relatively simple two element lens. The field within the lens causes the mass-separated beams to disperse without sacrificing resolution. Figure 5 presents a potential energy surface view of the EDL with a set of ion trajectories. Ions entering on the low mass side are accelerated as they enter the lens while ions entering on the high mass side are decelerated. Thus within the lens each isotope beam has a slightly different energy and thus is deflected through a different angle. At the exit all of the beams return to their initial energy. The EDL is physically located such that the focal point of the magnet is approximately at the center of the EDL; this produces the minimum broadening of each beam. The EDL was sized to accommodate 7 beams in the 230-250 amu mass range; the size could be changed to accommodate more or fewer beams.

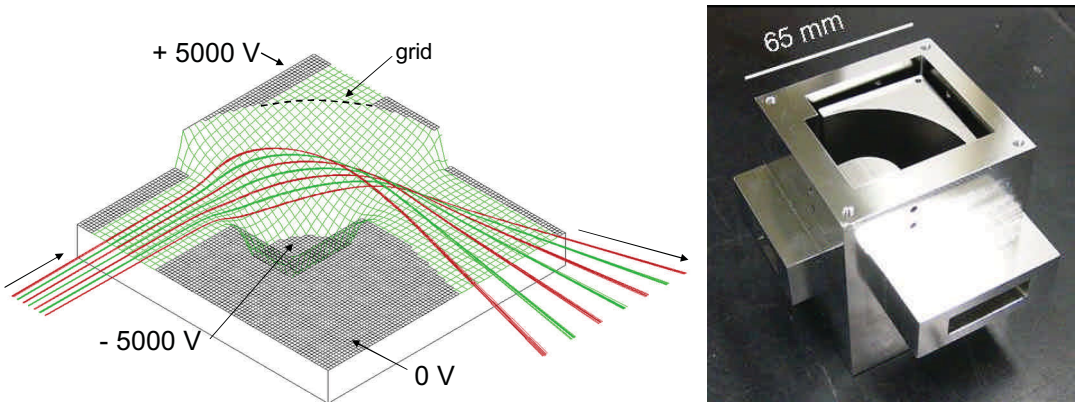

Figure 5 Potential energy surface view of the electrostatic dispersion lens and photograph. The mass separated beams enter on the left. The grid on the back electrode allows the ion beams to pass through the lens to a detector (not shown) when the electrodes are grounded.

Detector assemblies

The detector assemblies include a set of entrance optics for shaping and condensing the ion beam and the discrete dynode multipliers (photographs in following section). Figure 6 shows the ion optical model of the condenser lens with a set of ion trajectories. The lens is predicted to provide a factor of ~4.5 compression of the incoming ion beam.

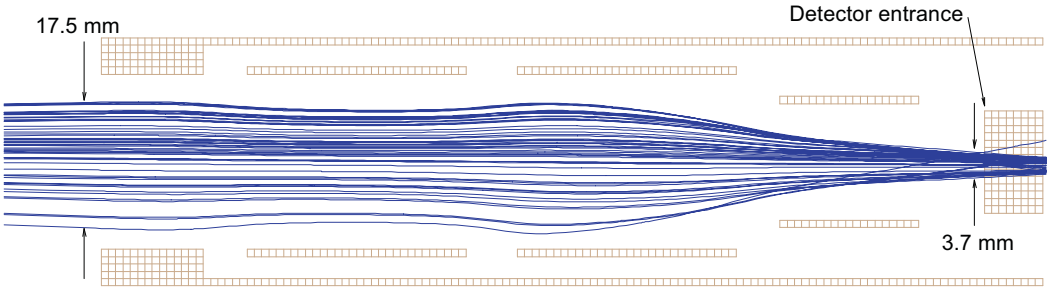

Figure 6 Detector entrance condenser lens with a set of ion trajectories. The detector entrance aperture is 7 x 11 mm.

Mechanical Design

The overall layout of the instrument as constructed and a photograph of the instrument are shown in Figures 7 and 8. Complete detailed mechanical drawings in AutoCad format were produced for all of the components and assemblies; part numbers and suppliers for all components not fabricated in-house are included on the drawings which are available on request.

Sample filaments are mounted in a 9-position cartridge that sits on an X-Z (side to side and up-down) micro-adjustable stage. The stage, powered by ultra-high-vacuum

compatible ceramic motors, can be moved in 10 μm increments horizontally and vertically, allowing the sample to be optimally positioned in the ion lens. Figure 9 shows photographs of the sample cartridge mounted in the vacuum chamber and the sample cartridge. A two-color pyrometer mounted on a viewport with a line of sight to the backside of the filament is used to monitor filament temperature. The source chamber is pumped with a single 270 l/s turbomolecular pump with an oil free backing pump; the typical operating pressure is 8 x 10^{-9} Torr.

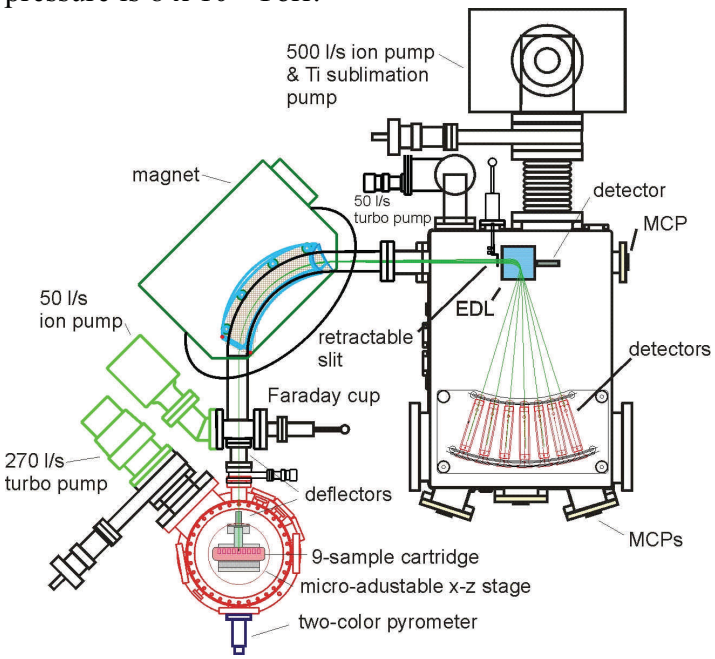

Figure 7 Physical layout of the instrument; footprint is 1.5 m x 1.5 m.

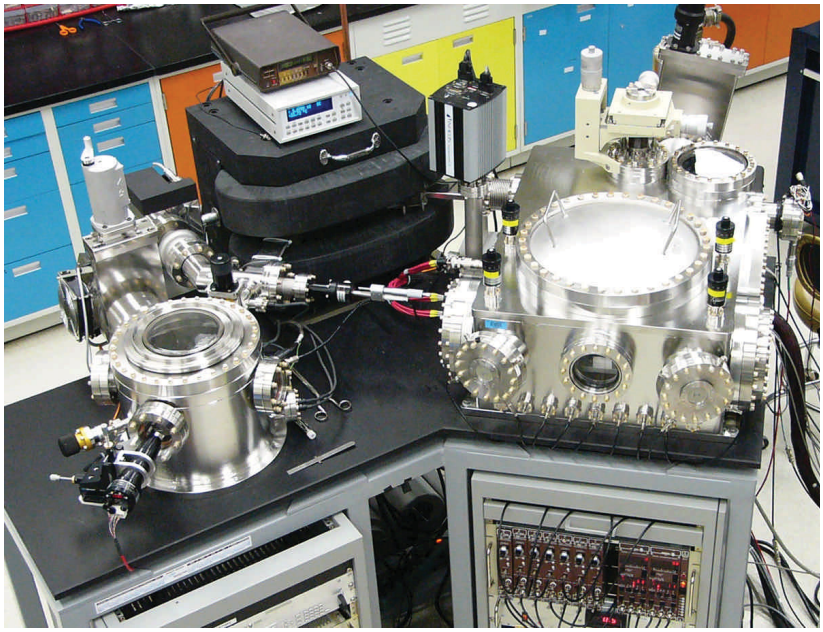

Figure 8 Photograph of the instrument, source chamber on the left, detector chamber on the right.

Two sets of two-axis beam deflectors are located between the ion lens and the magnet along with a retractable Faraday cup. The magnet is mounted on a platform that allows the height, tilt, and angular orientation to be adjusted relative to the flight tube. The flight tube contains a series of angled baffles coated with graphite attached on the inner and outer radius to reduce transmission of scattered ions. Figure 10 shows a photograph of a section of the baffle prior to installation. A 50 l/s ion pump is mounted on the flight tube at the entrance to the magnet.

At the exit of the magnet the ion beams pass into the detector chamber which contains the EDL and detectors (see Figure 7). The detector chamber is pumped with 500 l/s ion pump, a titanium sublimation pump, and a 50 l/s turbo pump with an oil free backing pump. The EDL contains two electrodes held at equal and opposite voltages and is mounted on a three axis manipulator so that its position can be adjusted from outside the vacuum chamber. A retractable slit is located just in front of the EDL; this can be used to operate the instrument in a single mass mode by setting the EDL voltages to zero so that the ion beam passes through the grid on the backside of the EDL (Figure 5) to a detector mounted on the EDL (Figure 7).

The detectors (ETP model AF150) are individually contained in separate enclosures that mount on a positioning dock. The positioning docks are mounted on a platform whose vertical position is adjustable from outside the vacuum system. The positioning docks can be moved on the platform to establish the required spacing between detectors and the detector enclosures can be removed from the positioning dock for detector replacement. This allows the detectors to be replaced without requiring realignment. Figure 11 shows photographs of the detector assemblies mounted on the platform and of a single detector in its housing. Figure 12 shows a CAD view of the detector condenser lens with the top cover removed.

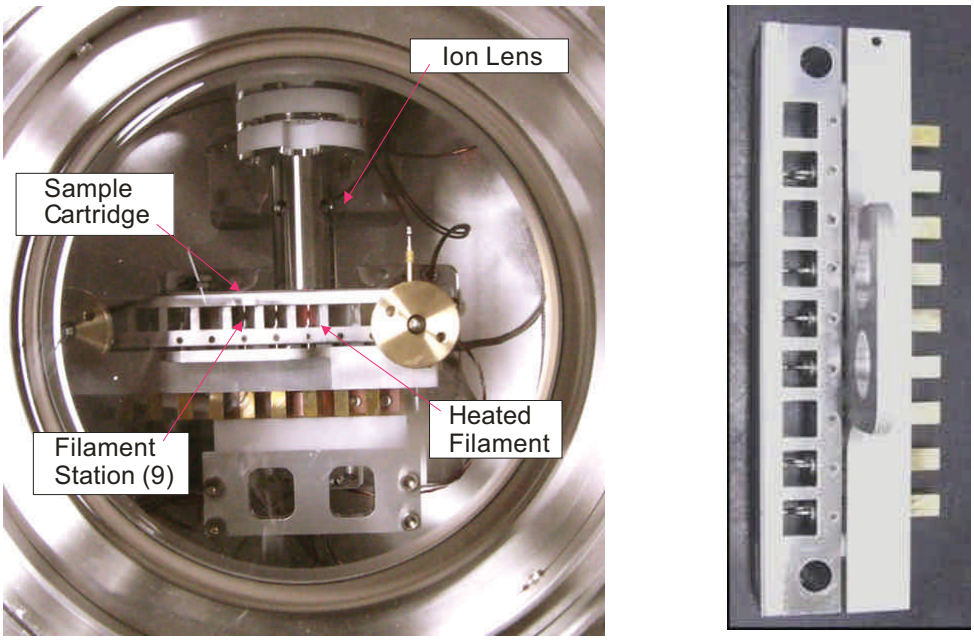

Figure 9 View through the top port of the source chamber (left) and the sample cartridge.

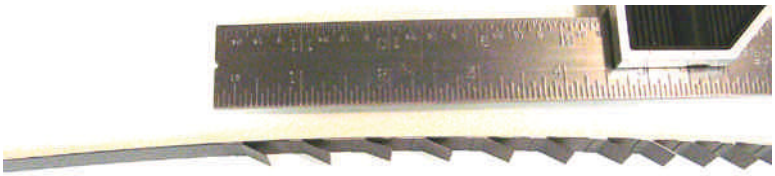

Figure 10 Section of the baffle liner placed in the flight tube to reduce scattered ions.

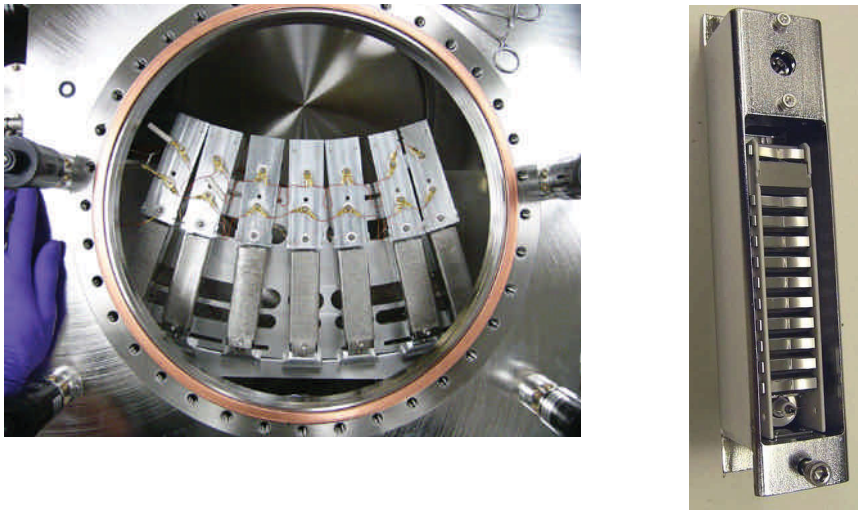

Figure 11 Photograph of the detectors with condenser lenses mounted on the adjustable platform in detector chamber (left) and (right) a detector mounted in its housing with the top screen removed.

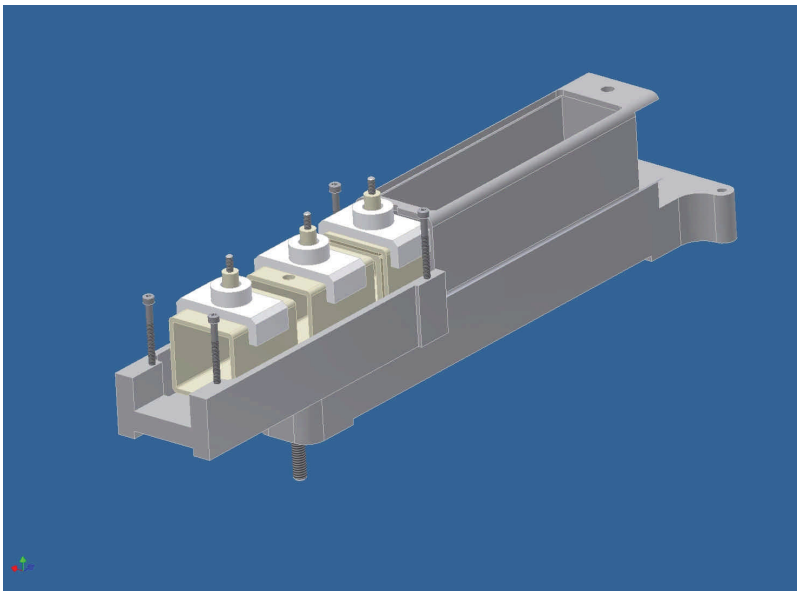

Figure 12 CAD drawing of the detector condenser lens; the top cover has been removed from the lens, and the detector is not shown in the housing.

Electronics and instrument control

The instrument is operated with a combination of computer and manual control of the electronics. Wherever practical the electronics are commercial units; all in-house fabricated electronics are documented with circuit diagrams and supplier lists. The instrument control and data acquisition software was written in LabVIEW and runs on a PC with communication to the electronics via IEEE-488, RS-232, and USB. The software is documented and maintained under INL quality level guidelines. Details are contained in the previous report[6] .

Performance Testing Results

To assess the performance of the instrument a series of samples produced at INL using SRM 996 (^{244}Pu spike) and SRM 4350B (Columbia River Sediment (CRS) were analyzed. The quantitative results obviously reflect both the performance of the instrument and of the sample processing and thus represent the current INL capability.

Sample Preparation

The ^{244}Pu spike solution was previously procured from Pacific Northwest National Laboratory from SRM 996 and used as received. Serial dilution was used as required to obtain the desired concentration. The samples were dried onto resin beads which were then mounted onto Re filaments (previously degassed at 4 amps). The mounted beads were carburized in a separate vacuum chamber using a slow ramp in temperature up to ~1400 C (2.3 amps) at which point a partial pressure of benzene of 5 e-5 Torr was established and held for 5 minutes. Typically, the samples were loaded in the mass spectrometer and analyzed within 2 days of carburization

The Columbia River Sediment samples were processed by dissolution of 10 g of the reference material using the standard method for these samples. Aliquots of the solution representative of a given mass of the reference material where then processed using the standard method and loaded onto resin beads which where then carburized using the method outlined above. 2.4 fg of ^{244}Pu spike was added to the samples at the start of the chemical processing and thus provided a measure of the overall yield of the chemistry and analysis, and quantitation of the 239 concentration.

Detector Cross Calibration

The 6 detectors used for these measurements were cross calibrated at least once each day that samples were analyzed. During the cross calibration the ^{244}Pu ion beam was directed into each detector using voltage switching; ten measurements of 2 s each were collected for each detector. The ten measurements for each detector were averaged and used to calculate the relative calibration factor for each detector. Figure 13 is a plot of the average and standard deviation (1 s , n = 60) of the calibration factor for each detector over the period the samples were analyzed. The count rates for calibration were kept at the level that is typically experienced during an analysis (200-1000 cps). While this introduces error due to low counting statistics it best represents the conditions encountered during an analysis.

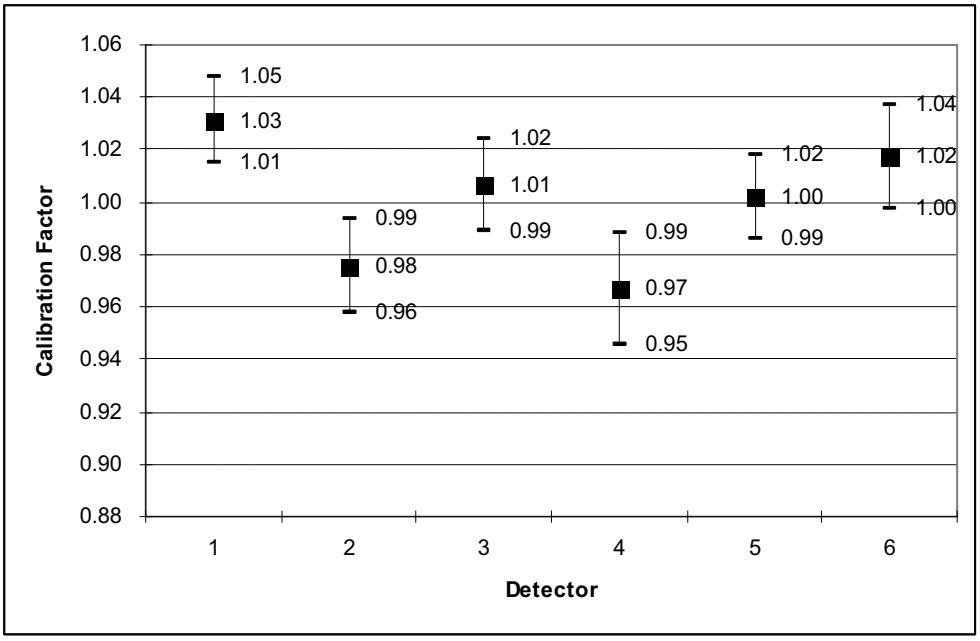

Figure 13 Average of the detector cross calibration factor and the standard deviation (1 s , n=60) for each of the detectors.

SRM 996 ^{244}Pu spike samples

Samples were prepared at two different loadings, 2.4 fg and 12 fg of ^{244}Pu, on resin beads which were then carburized as described previously. The mass spectrometer protocol was to heat the samples to ~1400 C and hold there for 4 minutes, during which the background count rate was measured, then to ramp the temperature in ~100 C increments at 30 s intervals to ~1800 C, at which point the sample position would be adjusted to maximize the signal intensity of ^{244}Pu, this typically took ~180 s, after which the sample temperature was increased to ~2150 C over ~20 s then held until the ^{244}Pu signal dropped to ~1 cps. Figure 14 illustrates a typical analysis for a 2.4 fg sample. The "noise" during the initial heating period (4 minutes) was typically from 2 to 7 counts per minute. The source chamber pressure during analysis was ~ 5 e-8 Torr and the detector chamber was 2 e-8 Torr.

The isotope ratios 242/244 and 240/244 were calculated using two methods; in one the background corrected ratio was calculated at each point in time (1 s intervals) over the selected time interval and the ratios were then averaged over the run. This method provided an estimate of the standard deviation of the ratio and thus of the standard error for the run. The second method was to sum the counts over the measurement period, subtract the background contribution and calculate the ratios; this does not provide an estimate of the ratio variation during the run. For the 12 fg samples the signal intensity is high enough that the background has essentially no effect on the ratio. However, for the 2.4 fg samples the signal level of the 240 isotope is low enough that the background can affect the ratio.

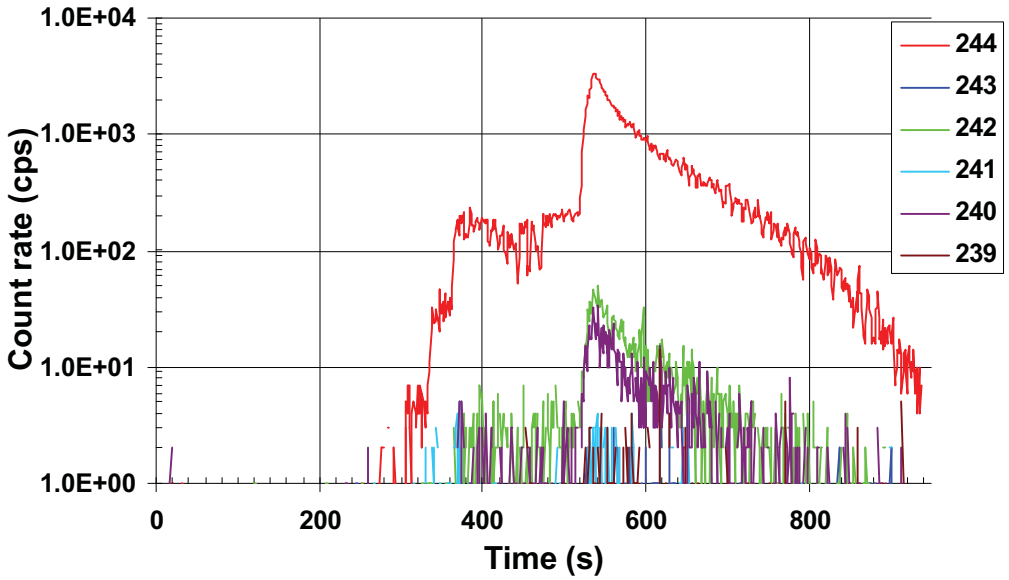

Figure 14 Typical signal for a 2.4 fg sample of SRM 996.

Table 1 and 2 present the measured isotope ratios, calculated using the count-rate method, and the sample utilization efficiencies for the 2.4 fg and 12 fg samples. The ratios have been normalized to the SRM 996 standard values corrected for decay. A counting system error was discovered in April in which low count rates (< 10 cps) were not being recorded accurately. Thus the ratios reported for the February-April data only include points where the count rate was >10 cps, the integrated count method was not applied, and no background subtraction was performed. Data for May-September were processed using both the count rate and the integrated count method and included background subtraction. Figures 15-18 display the 2.4 fg and 12 fg data from Table 1 and 2 in graphical format.

Table 1 Measured sample utilization efficiency (SUE) and isotope ratios normalized to the standard value for 2.4 fg of SRM 996 spike on resin beads; (242 = 33 attograms; 240 = 17 attograms).

No.	Date	SUE (%)	242/244	240/244
1	19-Feb	1.0	1.150	1.150
2	19-Feb	1.0	1.040	0.970
3	19-Feb	1.8	0.980	1.180
4	19-Feb	1.0	0.960	1.050
5	19-Feb	1.3	1.030	1.160
6	22-Feb	1.3	1.050	1.050
7	24-Feb	1.7	0.960	0.960
8	24-Feb	1.2	0.860	0.790
9	8-Mar	1.7	0.980	0.970
10	10-Mar	1.9	0.980	1.050
11	10-Mar	1.2	1.010	0.980
12	10-Mar	1.5	1.040	1.080
13	10-Mar	1.8	0.980	0.980
14	10-Mar	1.4	1.030	1.070
15	10-Mar	1.4	0.900	0.940
16	18-Mar	1.5	0.950	1.100
17	8-Apr	1.6	0.950	0.930
18	8-Apr	1.8	1.080	1.180
19	8-Apr	2.2	1.040	1.000
20	8-Apr	2.0	1.020	1.100
21	8-Apr	2.2	1.050	1.090
22	22-Apr	1.9	0.970	1.090
23	22-Apr	2.1	0.960	1.150
24	22-Apr	1.2	1.000	1.130
25	6-May	2.1	0.980	1.030
26	6-May	2.1	0.980	1.090
27	6-May	2.0	0.990	1.060
28	6-May	2.5	1.080	1.040
29	11-May	1.8	0.960	1.190
30	11-May	2.5	1.000	1.030
31	11-May	2.0	1.000	1.150
32	11-May	2.3	0.980	1.250
33	11-May	2.1	1.030	1.150
34	11-May	0.9	1.070	1.390
35	11-May	1.8	0.950	1.100
36	20-May	0.7	1.020	0.940
37	28-May	2.1	1.070	1.240
38	28-May	3.4	1.020	1.180
39	28-May	2.7	1.070	1.080
40	28-May	3.4	1.210	1.000
41	28-May	2.8	1.020	1.050
42	28-May	2.3	1.030	1.050
43	1-Jun	1.6	0.940	1.140
44	1-Jun	3.4	1.070	1.120
45	19-Aug	1.5	0.980	1.130
46	19-Aug	1.5	1.060	1.230
47	19-Aug	1.5	0.970	1.110

	Average	**1.837**	**1.010**	**1.083**
	Std. Dev.	**0.637**	**0.060**	**0.102**

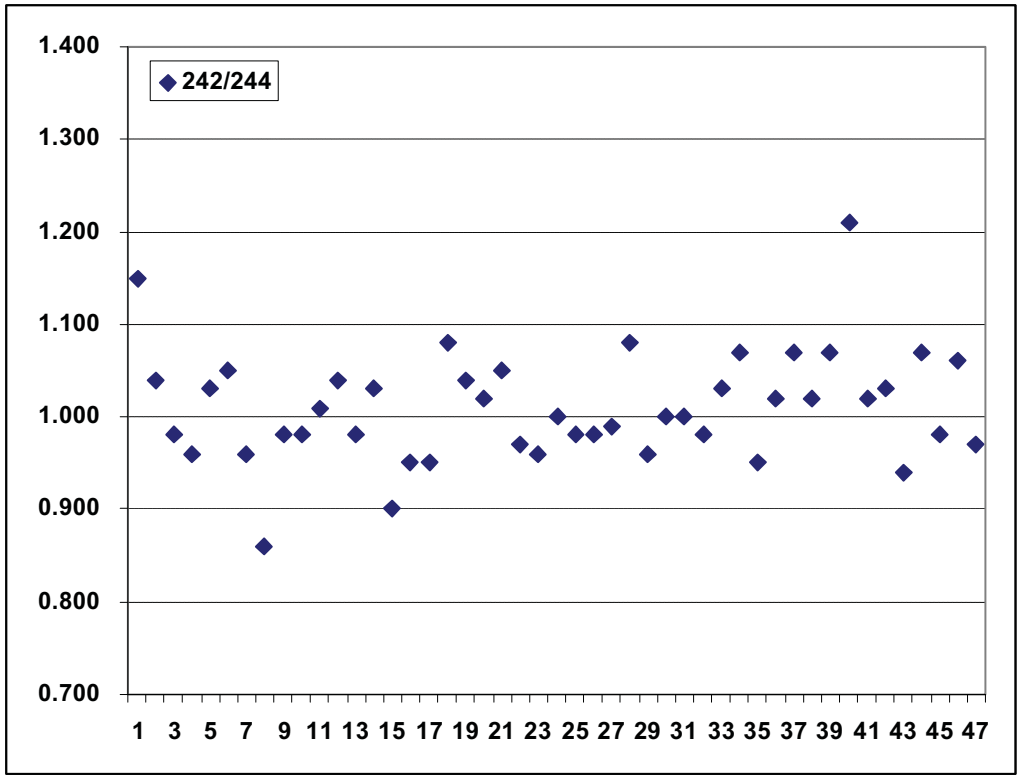

Figure 15 Isotope ratio normalized to the standard value for 2.4 fg ^{244}Pu samples (242 = 33 attograms).

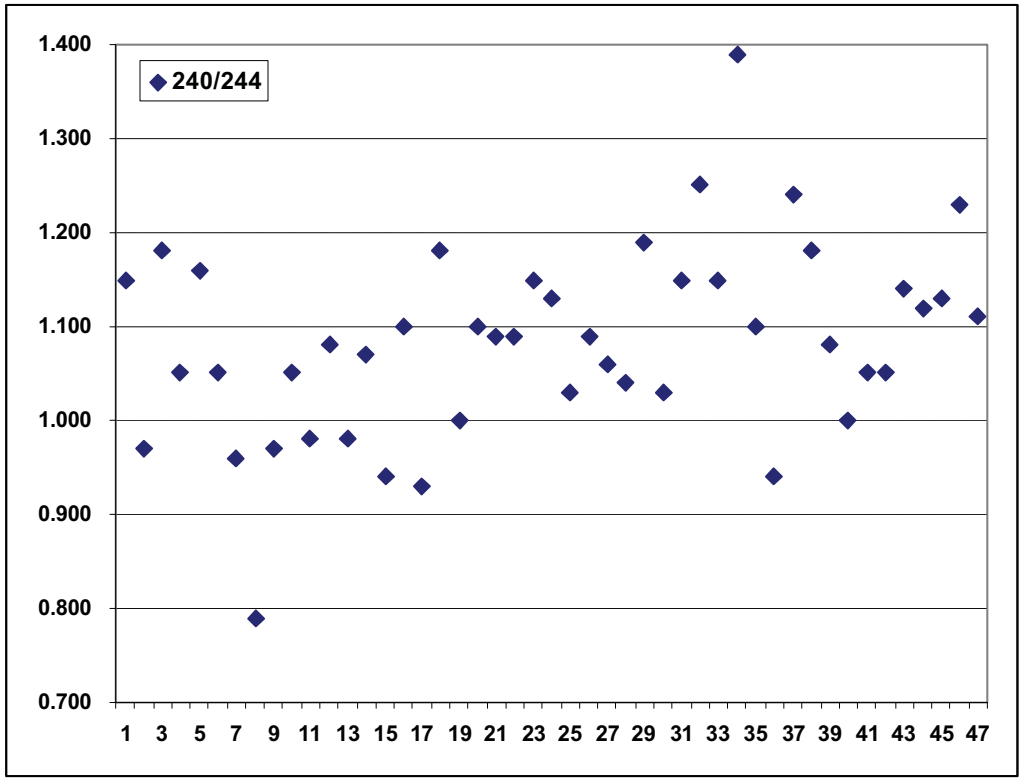

Figure 16 Isotope ratio normalized to the standard value for 2.4 fg ^{244}Pu samples (240 = 17 attograms).

Table 2 Measured sample utilization efficiency (SUE) and isotope ratios normalized to the standard value for 12 fg of SRM 996 spike on resin beads (242 =164 attograms; 240 = 84 attograms).

No.	Date	SUE 244	242/244	240/244
1	19-Feb	1.6	1.030	0.940
2	18-Mar	2.4	0.990	1.070
3	17-Mar	1.8	1.010	1.080
4	18-Mar	1.3	1.000	1.050
5	8-Mar	1.7	0.980	0.970
6	10-Mar	1.9	0.980	1.050
7	10-Mar	1.2	1.010	0.980
8	20-Apr	4.3	1.020	1.070
9	20-Apr	3.8	0.990	1.080
10	20-Apr	4.2	0.990	1.060
11	21-Apr	4.2	1.010	1.080
12	22-Apr	1.6	0.970	1.150
13	22-Apr	1.8	0.980	1.050
14	6-May	1.9	0.980	1.060
15	6-May	1.5	1.050	1.080
16	6-May	1.7	0.970	1.130
17	18-May	0.8	1.030	1.050
18	18-May	1.8	1.000	1.090
19	18-May	1.1	1.060	1.010
20	18-May	1.9	1.030	1.030
21	19-May	2.1	1.020	1.060
22	19-May	2.1	1.000	1.090
23	19-May	2.6	1.010	1.090
24	20-May	1.8	1.030	1.130
25	20-May	1.4	1.010	1.080
26	20-May	1.1	1.050	1.070
27	20-May	4.5	1.020	1.070
28	25-May	1.0	1.010	0.980
29	25-May	1.9	0.980	1.020
30	25-May	1.1	1.020	1.090
31	25-May	1.4	1.040	1.150
32	25-May	1.5	1.010	1.060
33	25-May	0.4	1.060	1.190
34	3-Jun	1.6	1.040	1.060
35	8-Jun	2.2	1.040	1.040
	Average	**2.0**	**1.012**	**1.065**
	Std Dev	**1.0**	**0.025**	**0.051**

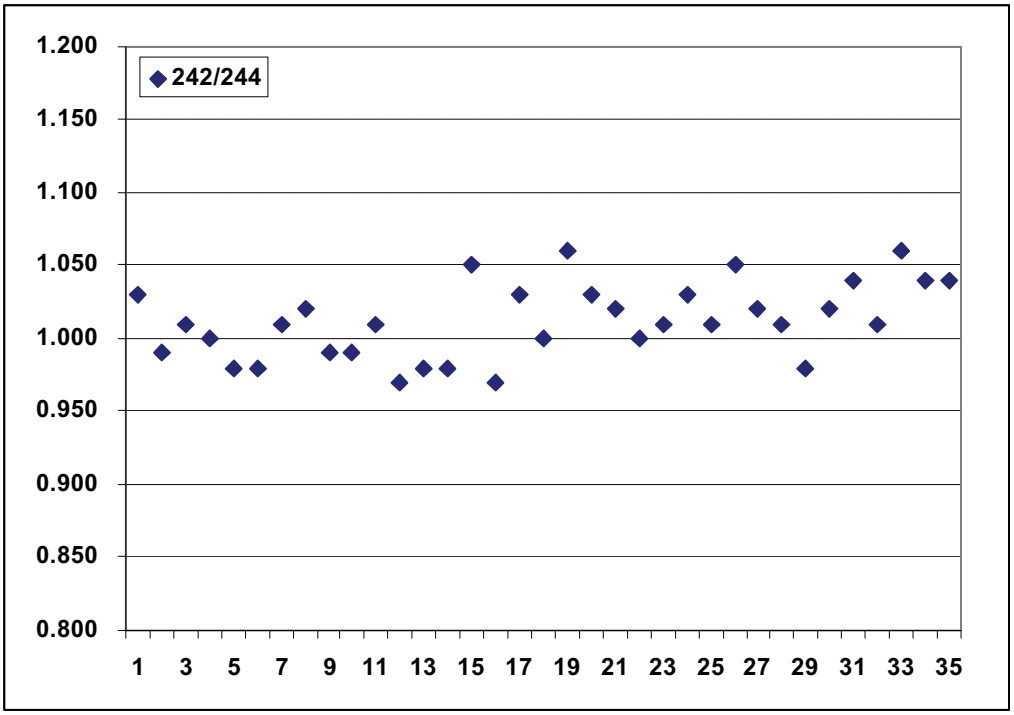

Figure 17 Isotope ratio normalized to the standard value for 12 fg ^{244}Pu samples (242 = 164 attograms).

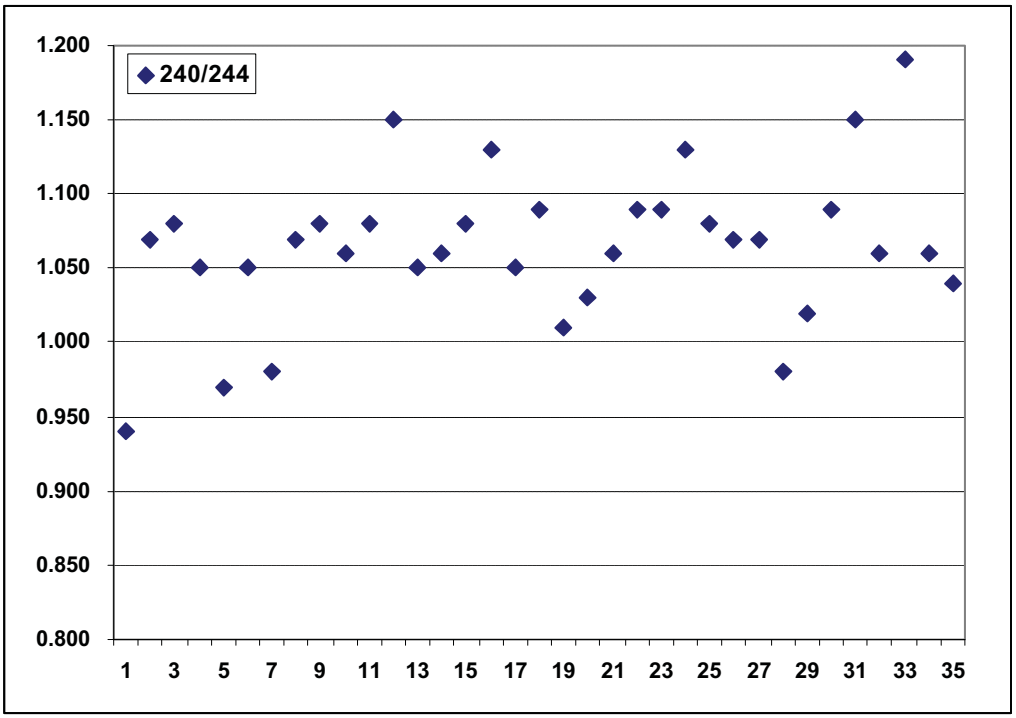

Figure 18 Isotope ratio normalized to the standard value for 12 fg ^{244}Pu samples (240 = 84 attograms).

The isotope ratios calculated using the count rate and the integrated count methods are compared in Table 3 for the 2.4 fg sample data from May-August and presented

graphically in Figures 19 and 20. Table 4 and Figures 21 and 22 present the same for the 12 fg samples. As expected the precision is significantly improved for the higher sample loading.

Table 3 Measured isotope ratios for 2.4 fg samples using the average-of-the-count-rate method and the total counts method. (242 = 33 attograms; 240 = 17 attograms)

No.	Date	count rate 242/244	total counts 242/244	count rate 240/244	total counts 240/244
1	6-May	0.980	0.990	1.030	1.070
2	6-May	0.980	0.990	1.090	1.050
3	6-May	0.990	1.010	1.060	1.100
4	6-May	1.080	1.090	1.040	1.040
5	11-May	0.960	0.920	1.190	1.110
6	11-May	1.000	0.960	1.030	1.040
7	11-May	1.000	0.970	1.150	1.080
8	11-May	0.980	0.930	1.250	1.230
9	11-May	1.030	0.950	1.150	1.010
10	11-May	1.070	0.990	1.390	1.240
11	11-May	0.950	0.960	1.100	1.040
12	20-May	1.020		0.940	
13	28-May	1.070	1.040	1.240	1.090
14	28-May	1.020	1.020	1.180	1.110
15	28-May	1.070	1.060	1.080	1.090
16	28-May	1.210	1.140	1.000	1.000
17	28-May	1.020	0.980	1.050	1.030
18	28-May	1.030	1.020	1.050	1.010
19	1-Jun	0.940	0.840	1.140	1.140
20	1-Jun	1.070	1.060	1.120	1.130
21	19-Aug	0.980	1.000	1.130	1.120
22	19-Aug	1.060	1.010	1.230	1.170
23	19-Aug	0.970	0.980	1.110	1.140
	Average	**1.021**	**0.996**	**1.120**	**1.093**
	Std. Dev.	**0.059**	**0.062**	**0.098**	**0.066**

Table 4 Measured isotope ratios for 12 fg samples using the average-of-the-count-rate method and the total counts method (242 =164 attograms; 240 = 84 attograms).

No.	Date	count rate 242/244	total counts 242/244	count rate 240/244	total counts 240/244
1	20-May	1.030	1.04	1.130	1.12
2	20-May	1.010	1.02	1.080	1.05
3	20-May	1.050	1.03	1.070	1.08
4	20-May	1.020	1	1.070	1.04
5	25-May	1.010	0.98	0.980	1.03
6	25-May	0.980	0.97	1.020	1.02
7	25-May	1.020	1.02	1.090	1.06
8	25-May	1.040	1.03	1.150	1.1
9	25-May	1.010	1.03	1.060	1.04
10	25-May	1.060	1.04	1.190	1.13
11	3-Jun	1.040	1.01	1.060	1.05
12	8-Jun	1.040	1.04	1.040	1.03
	Average	**1.026**	**1.018**	**1.078**	**1.063**
	Std Dev	**0.022**	**0.023**	**0.057**	**0.037**

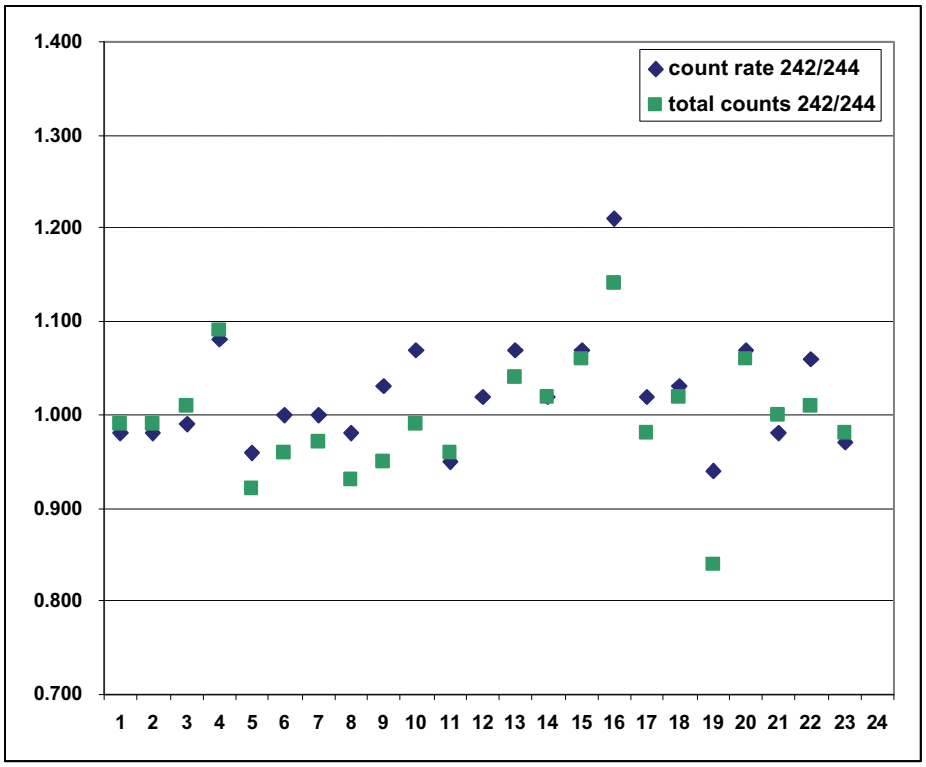

Figure 19 Comparison of count rate and total counts methods for calculating isotope ratios for the 2.4 fg samples (242 = 33 attograms).

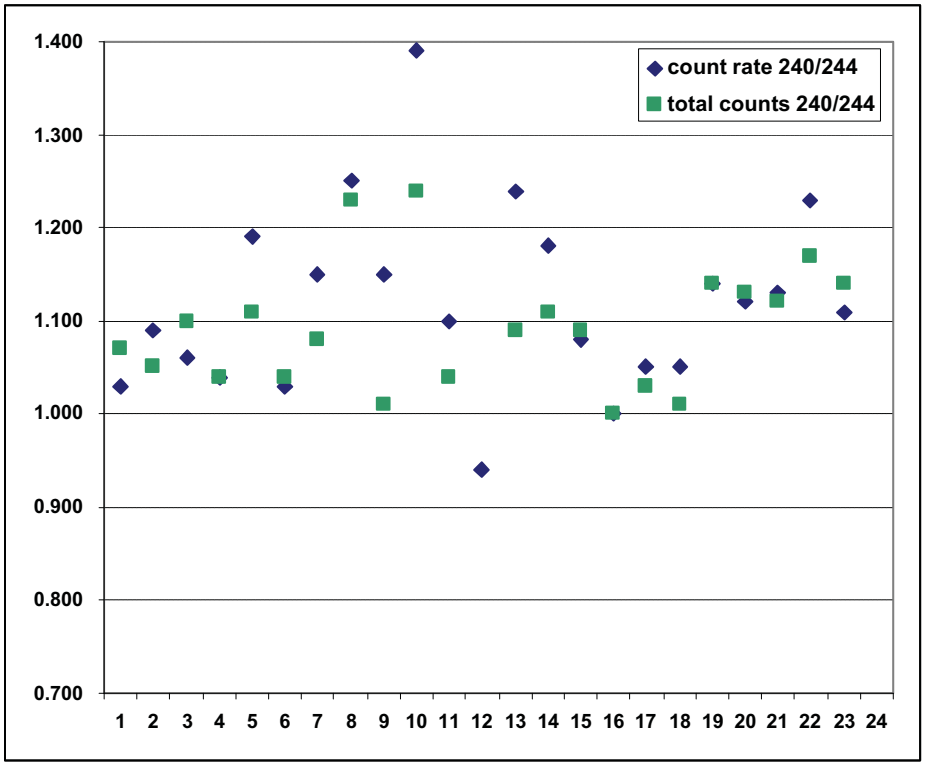

Figure 20 Comparison of count rate and total counts methods for calculating isotope ratios for the 2.4 fg samples (240 = 17 attograms).

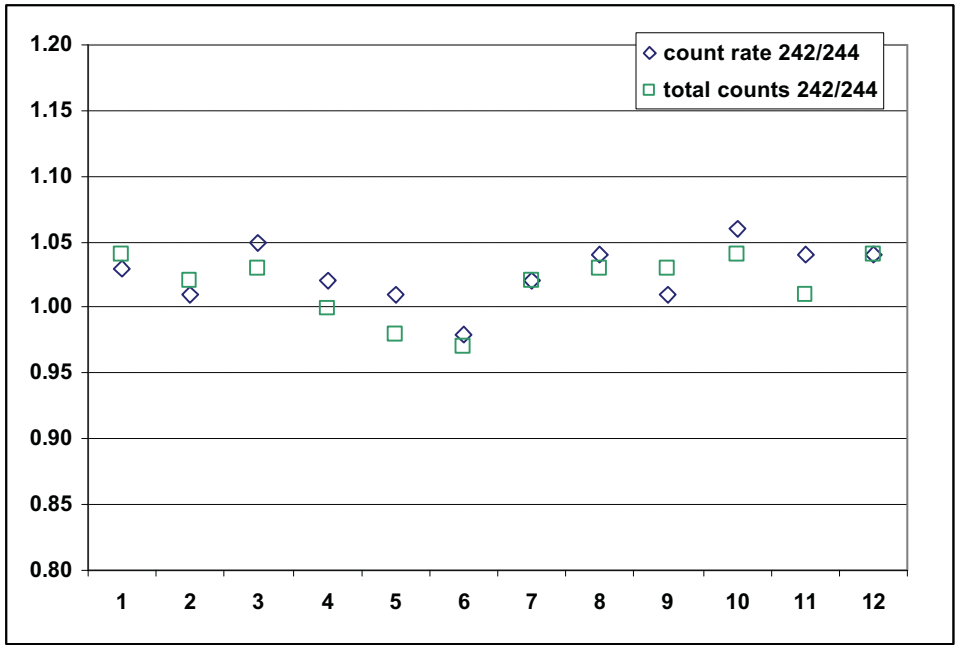

Figure 21 Comparison of count rate and total counts methods for calculating isotope ratios for the 12 fg samples (242 =164 attograms).

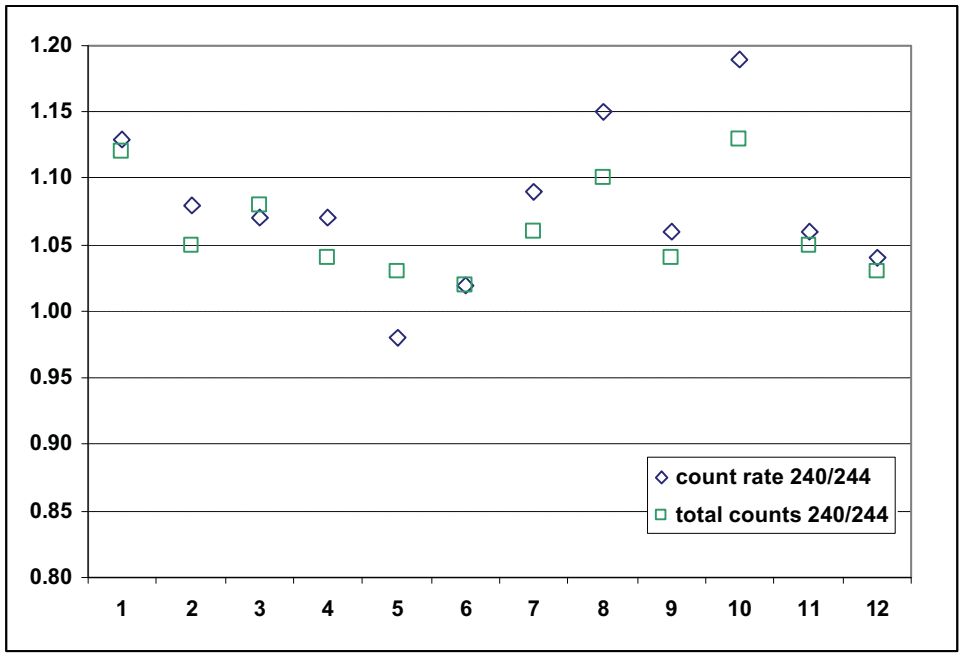

Figure 22 Comparison of count rate and total counts methods for calculating isotope ratios for the 12 fg samples (240 = 84 attograms).

The limit of detection (LOD) can be estimated from the standard deviation and is typically defined as 3 s . From Table 3 the LOD for the 240 isotope is 3.3 attograms for the total count method and 5.0 attograms for the count rate method.

The limit of quantitation (LOQ) is defined at 10 s , and thus for the 240 isotope (Table 3) is 11.2 attograms for the total count method and 16.7 attograms for the count rate method.

SRM 4350B Columbia River Sediment samples

Two sets of Columbia River Sediment samples and 2 process blanks were prepared and analyzed. For all samples the "noise" during the initial heating period (4 minutes) was typically from 2 to 7 counts per minute. The source chamber pressure during analysis was ~ 5 e-8 Torr and the detector chamber was ~2 e-8 Torr.

The starting sample sizes for the sample sets were 17 and 1 mg/sample; SRM 996 spike was added at the beginning of chemical processing for quantification of the yield. Samples were prepared at a loading of 2.7 fg ^{239}Pu (assuming 100% yield) from the sample and 2.4 fg ^{244}Pu from the spike for the 17 mg samples, and 174 attograms ^{239}Pu from the sample and 2.4 fg ^{244}Pu spike for the 1 mg samples. The loaded resin beads were carburized as described previously. The mass spectrometer protocol was to heat the samples to ~1400 C and hold there for 4 minutes, during which the background count rate was measured, then to ramp the temperature in ~100 C increments at 30 s intervals to ~1800 C, at which point the sample position was adjusted to maximize the signal intensity of ^{244}Pu, this typically took ~180 s, after which the sample temperature was increased to the maximum temperature (~ 1950 C) over ~20s then held until the ^{244}Pu signal dropped to <10 cps. The maximum temperature was lower than used for the SRM 996 samples because an interference appeared at mass ^{244}Pu at higher temperatures.

Figure 23 illustrates a typical analysis and Table 5 presents the results for all samples. The theoretical concentration of 239 was calculated to be 160 fg/g based on the activity level of the starting material in the standard; the average measured concentration was 152 +/- 6 fg/g with a slightly higher uncertainty for the 1 mg samples. Also included in Table 5 are the results for a sample in which only 296 atoms of ^{239}Pu were measured; the measured concentration of ^{239}Pu for that sample was 188 fg/g, within 17% of the theoretical value.

The average ^{239}Pu level (background subtracted) in the process blanks (Table 5) was 3% of the average signal level for the lowest concentration sample (1 mg), and 0.3% of the average signal level of the 17 mg samples.

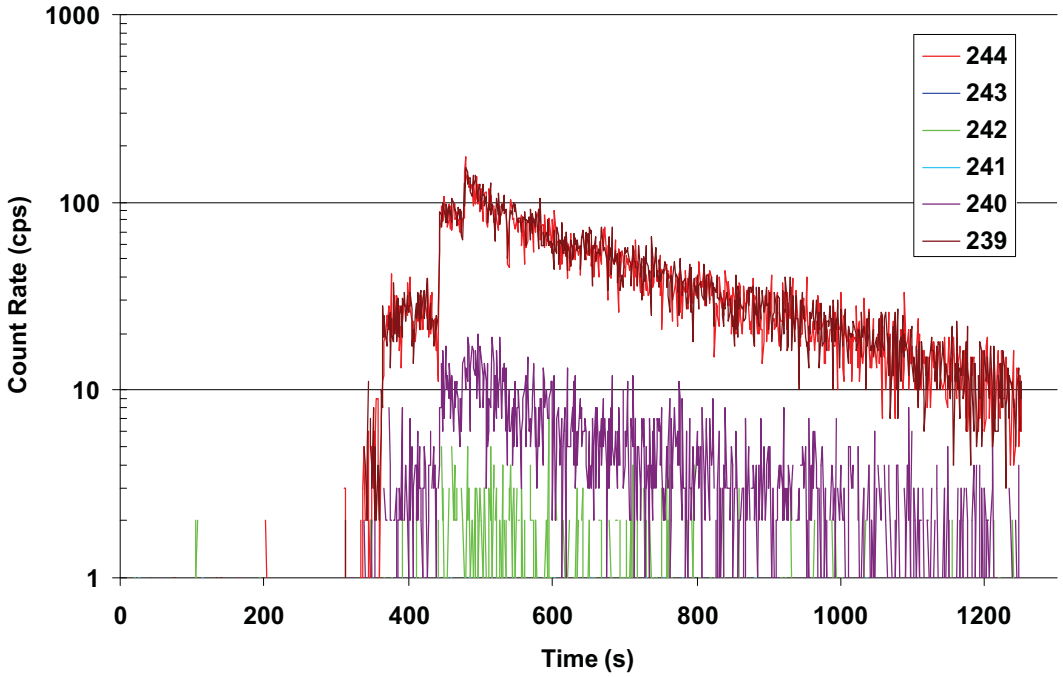

Figure 23 Ion signal for a typical SRM 4350B CRS sample loaded with a theoretical total of 5.1 fg of Pu (2.4 fg from spike and 2.7 fg from CRS sample assuming 100% chemistry yield).

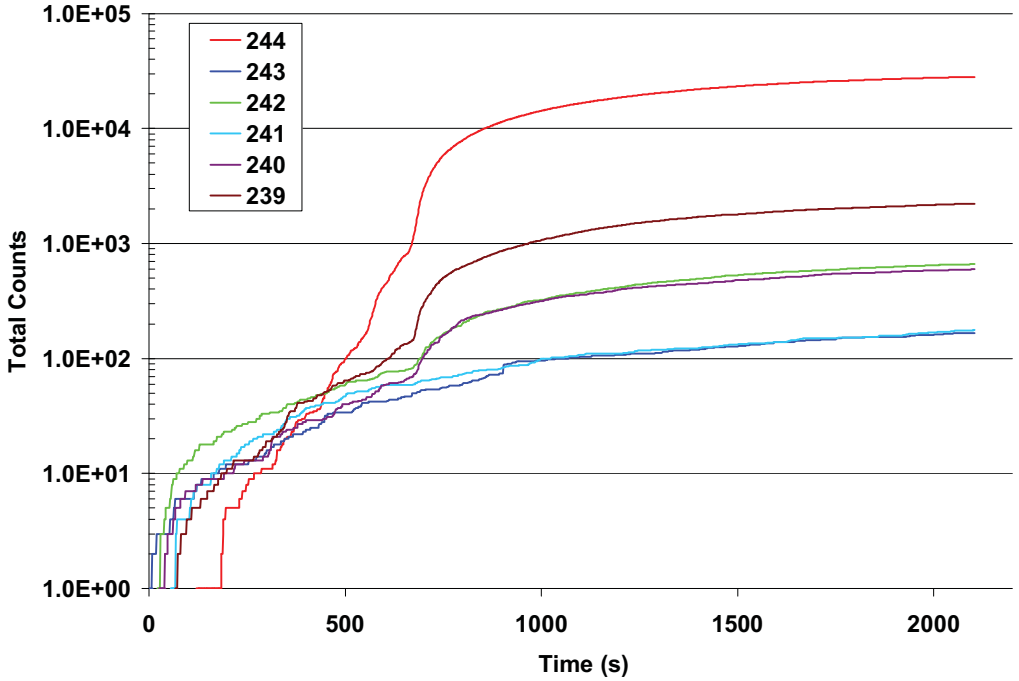

Figure 24 Integrated counts for a typical 0.001 g sample; maximum filament temperature 1972 C.

Table 5 Columbia River Sediment Sample Results

Date	Extractred Sample Size (g)	239 Atoms Detected	SUE 244 (%)	242/239 (meas./std.)	240/239 (meas./std.)	244/239 (meas./std.)	fg/g 239
5-Aug	0.0169	21,727	0.35	1.07	0.97	1.11	147
5-Aug	0.0169	29,371	0.48	0.91	0.98	1.12	146
5-Aug	0.0169	11,906	0.19	0.92	0.93	1.11	148
5-Aug	0.0169	24,853	0.40	0.92	0.97	1.11	147
5-Aug	0.0169	17,641	0.27	0.94	0.98	1.07	153
10-Aug	0.0169	25,936	0.42	1.11	0.98	1.13	150
17-Aug	0.0169	15,328	0.25	1.02	0.96	1.07	160
17-Aug	0.0169	50,164	0.77	1.14	0.94	1.09	159
3-Sep	0.0169	22,164	0.36	0.95	1.07	0.95	156
	average	**24,344**	**0.39**	**1.00**	**0.98**	**1.08**	**152**
	std dev (1-s)	**11,109**	**0.17**	**0.09**	**0.04**	**0.05**	**6**
18-Oct	0.0011	2,603	0.69	1.21	1.14	1.16	142
18-Oct	0.0011	2,711	0.67	1.03	1.27	1.08	151
18-Oct	0.0011	1,446	0.37	1.32	1.37	1.11	147
19-Oct	0.0011	1,618	0.38	1.16	1.39	1.04	157
20-Oct	0.0011	1,990	0.46	1.14	1.23	1.02	162
	average	**2,074**	**0.51**	**1.17**	**1.28**	**1.08**	**152**
	std dev (1-s)	**569**	**0.16**	**0.11**	**0.10**	**0.06**	**8**
19-Oct	0.0011	296	0.06	0.99	2.07	0.87	188
20-Oct	proc blank	33	0.21				
20-Oct	proc blank	117	0.47				

Conclusion

The performance of the instrument was measured using SRM 996 (^{244}Pu spike) at loadings of 2.4 and 12 fg on resin beads and with the SRM 4350B Columbia River Sediment standard. The measured limit of detection (3s) for ^{240}Pu was 3.4 attograms for SRM 996. The limit of quantitation, defined as 10s, was 11.2 attograms. The measured concentration of ^{239}Pu in the CRS standard was 152 ± 6 fg/g.

REFERENCES

1 N. R. Daly, Rev. Sci. Instrum. 31 (1960) 264.
2 M. E. Wieser and Johannes B. Schwieters, Int. J. Mass Spectrom. 242 (2005) 97-115.
3 Nu Instruments Ltd, Wrexham LL13 9XS North Wales, UK; www.nu-ins.com
4 IsotopX Ltd, Middlewich Cheshire CW10 0GE UK
5 Thermo-Scientic, Waltham, MA 02454, USA
6 Multi-collector Isotope Ratio Mass Spectrometer – Design, Fabrication and Operational Testing Preliminary Report, INL internal report, November 2008.
7 United States patent number 6,984,821, Jan. 10, 2006. Additional patent pending.
8 Appelhans, A. D.; Olson, J. E.; Delmore, J. E.; *Int J Mass Spec*, 241 (1) 1-9 (2005).
9 D. A. Dahl, A. D. Appelhans, M. B. Ward, Int. J. Mass Spectrom. Ion Process.189 (1999) 47-51.
10 D. A. Dahl, Int. J. Mass Spectrom. 200 (2000) 3-25.
11 VG corporation, now IsotopX; www.IsotopX.co.uk